

Broadening of the thermal component of the prompt GRB emission due to rapid temperature evolution

Priya Bharali^{a,d}, Sunder Sahayanathan^b, Ranjeev Misra^c, Kalyanee Boruah^d

^a*Girijananda Chowdhury Institute of Management and Technology, Guwahati, India*

^b*Bhabha Atomic Research Centre, Mumbai, India*

^c*IUCAA, Pune, India*

^d*Department of Physics, Gauhati University, Guwahati, India*

Abstract

The observations of the prompt emission of gamma ray bursts (GRB) by GLAST Burst Monitor (GBM), on board *Fermi* Gamma-ray Space Telescope, suggest the presence of a significant thermal spectral component, whose origin is not well understood. Recently, it has been shown that for long duration GRBs, the spectral width as defined as the logarithm of the ratio of the energies at which the spectrum falls to half its peak value, lie in the range of 0.84-1.3 with a median value of 1.07. Thus, while most of the GRB spectra are found to be too narrow to be explained by synchrotron emission from an electron distribution, they are also significantly broader than a blackbody spectrum whose width should be 0.54. Here, we consider the possibility that an intrinsic thermal spectrum from a fire-ball like model, may be observed to be broadened if the system undergoes a rapid temperature evolution. We construct a toy-model to show that for bursts with durations in the range 5-70 seconds, the widths of their 1 second time-averaged spectra can be at the most $\lesssim 0.557$. Thus, while rapid temperature variation can broaden the detected spectral shape, the observed median value of ~ 1.07 requires that there must be significant sub-photospheric emission and/or an anisotropic explosion to explain the broadening for most GRB spectra.

Keywords: gamma rays: bursts - radiation mechanisms: thermal - relativity

Email addresses: priya_phy@gimt-guwahati.ac.in (Priya Bharali), sunder@barc.gov.in (Sunder Sahayanathan)

1. Introduction

Gamma ray bursts (GRB) are the most luminous, transient phenomena happening in the universe with luminosities of the order of $10^{51} - 10^{52}$ erg/s (Piran, 2004). The prompt phase of the GRB corresponds to the initial episodic event which lasts typically for a duration ranging from a fraction of a second to few tens of seconds. This is often followed by a fading emission, long after the initial burst decayed, termed as “after glow”. Optical study of these after glow confirmed the cosmological origin of GRBs (Costa et al., 1997; van Paradijs et al., 1997). The distribution of the burst duration of GRBs is bimodal with a minima falling at ~ 2 s suggesting the GRB may plausibly arise from two different process (Kouveliotou et al., 1993). Accordingly they were classified into two types, namely short bursts with duration < 2 s and long bursts with duration > 2 s. Further, the spectra of short bursts are typically harder than the long ones supporting different origin of these two classes (Bhat et al., 2016; Kouveliotou et al., 1996; Dezalay et al., 1996). The progenitor of the GRBs are not well understood; however, observational and theoretical advancements suggests short GRBs to be associated with the mergers of compact objects, e.g. neutron star-neutron star merger or neutron star-black hole merger (Eichler et al., 1989; Paczynski, 1991; Rosswog, Piran, & Nakar, 2013), and the long ones are associated with the collapse of a massive star onto a black hole (Woosley, 1993; MacFadyen & Woosley, 1999).

Initial attempts to understand the GRB emission were focussed on thermal nature originating from a catastrophic event involving collapse of a massive star or merging of two compact objects (Paczynski, 1986; Goodman, 1986). The huge energy released within a small volume implies, the optical depth of the initial medium to be very high and the interaction between the energetic photons and particles will cause the medium to expand at relativistic speed, commonly referred as “fire-ball”. However, after sufficient expansion, the fire-ball approaches the photospheric stage where further decrease in density transits the matter to optically thin regime and the trapped thermal photons are released (Goodman, 1986; Burgess & Ryde, 2015). On the contrary, the time-averaged spectra of GRBs, observed by *BATSE* on board *CGRO*, are found to be non-thermal and are well explained by a broken power-law function with smooth transition at the break frequency (Band function) (Band et al., 1993). To understand this non-thermal emission, internal

shock models were proposed where particles are accelerated at a shock front initiated by the collision between shells of matter expelled by the initial catastrophic event (Kobayashi, Piran, & Sari, 1997; Panaitescu & Meszaros, 1998; Daigne & Mochkovitch, 1998). The GRB emission is then modelled as the synchrotron emission from the relativistic electron population accelerated at these shock fronts. Alternatively, Blinnikov, Kozyreva, & Panchenko (1999) showed that a non-thermal spectrum can also be imitated by the time integration of blackbody emission arising from an evolving GRB shells.

The observed photon spectral indices of many GRBs; however, confront the synchrotron emission interpretation as the indices are steeper than the one allowed by this model (Crider et al., 1997; Preece et al., 1998; Ghirlanda, Celotti, & Ghisellini, 2003). In addition, the low energy conversion efficiency of internal shock models posed severe drawback (Ryde, 2004; Pe'er & Ryde, 2016). These discrepancies forced the addition of a thermal component in the GRB spectra again, along with the non-thermal one (Guiriec & Fermi/GBM Collaboration, 2010; Guiriec et al., 2013; Zhang & Yan, 2011; Burgess et al., 2014; Axelsson et al., 2012). After the advent of *Fermi* and *Swift*, satellite based experiments operating at gamma ray and X-ray energies, the presence of thermal component in GRB spectrum became more evident (Basak & Rao, 2014; Rao et al., 2014).

Recently, Axelsson & Borgonovo (2015) performed an elaborative spectral study of long and short bursts observed by Fermi/GBM and CGRO/BATSE and compared their spectral widths. The full width half maximum (W) of the EF_E representation of the spectra, with E being the photon energy and F_E the specific flux, was calculated during the flux maximum of each bursts by fitting the observed fluxes using a Band function. Interestingly, the width distribution peaked at ~ 1.07 for long GRBs and ~ 0.86 for short GRBs, which is much broader than the Planck function ($W \approx 0.54$) but narrower than the synchrotron spectrum due to a Maxwellian distribution of electrons ($W = 1.4$) or a power-law electron distribution with index -2 ($W = 1.6$). A similar study was also carried out by Yu et al. (2015) who studied the spectral curvature at the peak of the GRB spectrum for 1113 bursts detected by the *Fermi* GBM experiment. Again, they concluded that most of the bursts are inconsistent with synchrotron emission models or a single temperature blackbody emission. In case of short bursts, a detailed study of spectral broadening was performed by Bégué & Vereshchagin (2014) using approximate analytical solution for the relativistic

hydrodynamic equations.

In the present work, we study the broadening of the photospheric thermal emission due to relativistic effects under the fire-ball model of GRBs. We consider a scenario where the temperature of the fire-ball decreases rapidly with increase in radius and this causes the high latitude emission to be relatively hotter than the on-axis emission for a distant observer. In addition, the time integrated spectrum will cause further broadening due to the evolution of the fire-ball within the integration time. Particularly, we investigate the maximum attainable width of this multi temperature black-body emission within the burst timescale typical for long GRBs. In the next section, we describe the model and the spectral properties. In §3, we study the maximum attainable width under the present model for the case of long GRBs and summarize the work in §4.

2. Spectral Evolution of an Expanding Fire-ball

We consider the thermal emission from the photosphere of GRB to be associated with the release of radiation trapped in an initial optically thick and relativistically expanding ball of plasma (Fire-ball). We also assume the expansion to be associated with a rapid fall in temperature described by

$$T(r) = T_0 \left(\frac{r_0}{r} \right)^\psi \quad (1)$$

Here, T is the temperature when the fire-ball radius is r , T_0 corresponds to the temperature at radius r_0 and ψ is the temperature index describing the cooling. The burst is assumed to be in its coasting phase and hence the expansion velocity will be approximately constant till the internal shock or other dissipative events occur (Vedrenne & Atteia, 2009). Further, if the expansion is adiabatic, conservation of entropy limits the value of ψ to be $2/3$ during the coasting phase of the burst (Piran, Shemi, & Narayan, 1993; Pe'er, 2015).

The relativistic expansion of the fire-ball and the light travel time effect will cause the emission from a higher latitude to be hotter than the on axis emission for a distant observer. The flux at frequency ν received by the observer located at a distance D will then be a modified blackbody

spectrum given by (Appendix Appendix A)

$$f_\nu(r_0) = \frac{4\pi h}{c^2} \frac{r_0^2}{D^2} (1 - \beta)^2 \nu^3 \int_{\beta}^1 \frac{\mu d\mu}{\left\{ \exp \left[\frac{h\nu}{\Gamma k T_0 (1 + \beta\mu)} \left(\frac{1 - \beta}{1 - \beta\mu} \right)^\psi \right] - 1 \right\}} \frac{(\mu - \beta)}{(1 - \beta\mu)^3} \quad (2)$$

where, β is the expansion velocity in units of the speed of light c and $\Gamma = (1 - \beta^2)^{-1/2}$ is the corresponding Lorentz factor, r_0 is the on axis radius of the fire-ball measured by the observer, μ is the cosine of the latitude, h is the Planck constant and k is the Boltzmann constant. If we consider the photosphere to be spherical, then the relativistic beaming effects will cause the off-axis emission received by the observer to be limited within an angle $1/\Gamma$ subtended at the centre of the fire-ball. When the comoving plasma density varies as r^{-2} and for an energy independent photon scattering cross section, the photosphere can be significantly different from a simple sphere (Abramowicz, Novikov, & Paczynski, 1991). However, within the opening angle $1/\Gamma$ along the line of sight of the observer, the surface of the photosphere can still be approximated as spherical (Pe'er, 2008). For simplicity, the photosphere emission beyond this angle is not considered in the present work. In Fig. 1, we show the instantaneous spectrum (normalized) for $\Gamma = 500$, $\psi = 2/3$ and $T_0 = 10$ keV along with equivalent blackbody spectrum. For $\Gamma \gg 1$, as in the case of GRBs, the emission cone will be narrower and the instantaneous spectrum observed will drift towards a simple blackbody, unless ψ is large enough to create significant off-axis temperature variation.

Following Axelsson & Borgonovo (2015), if we define the width of the resultant spectrum as (Fig. 1)

$$W = \log \left(\frac{\nu_2}{\nu_1} \right) \quad (3)$$

where, ν_1 and ν_2 are the photon frequencies at the full width at half maximum (FWHM) of the νf_ν (unit: $ergs/cm^2/s$) spectrum, then for $\psi > 0$, W will be larger than the one expected from a simple blackbody spectrum ($W \approx 0.54$). In addition, for $\Gamma \gg 1$, W will depend mainly on ψ and in Fig. 2 we show its variation with respect to the latter. As ψ increases, W increases from ~ 0.54 to a maximum of ≈ 0.675 corresponding to $\psi \approx 2.7$. Beyond this, the temperature gradient becomes too large such that the on-axis emission fall below the FWHM of the hotter high latitude emission, causing W to decrease with further increase in ψ . Under the adiabatic limit ($\psi = 2/3$),

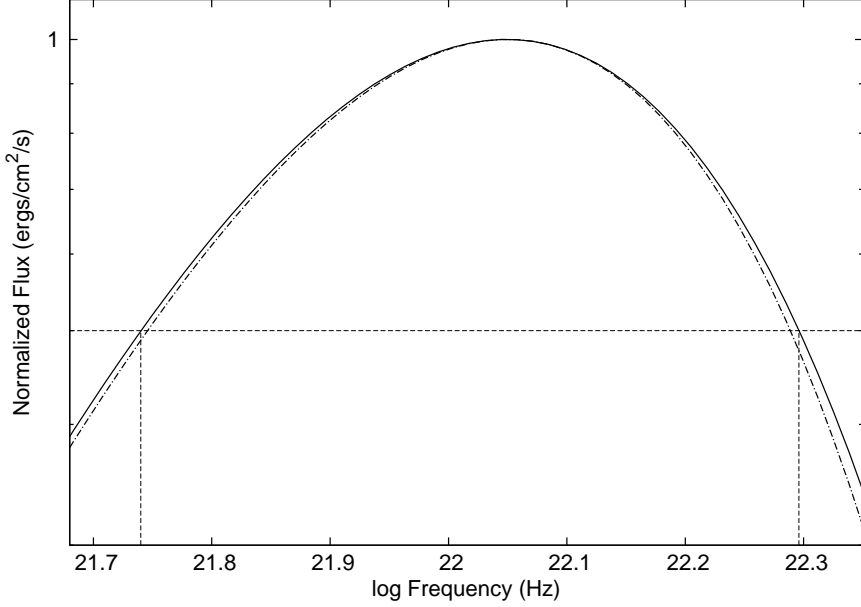


Figure 1: The instantaneous spectrum corresponding to $\Gamma = 500$ and $\psi = 2/3$ for $T_0 = 10$ keV. The dashed line indicates the spectral width W measured at FWHM. The dot-dashed line represents equivalent blackbody spectrum.

the maximum value of W that can be attained is ≈ 0.556 and beyond this range is shown as the shaded region in Fig. 2.

A time-averaged spectrum will involve the temporal evolution of the fire-ball within the duration and this will further broaden the spectrum. Considering the fire-ball expands from a radius r_1 to r_2 during an interval, the time-averaged spectrum will then be

$$F_{1,2}(\nu) = \frac{\int_{r_1/r_2}^1 \bar{f}_\nu(x) dx}{1 - r_1/r_2} \quad (4)$$

where, $\bar{f}_\nu(x) = f_\nu(xr_2)$ and the corresponding temperature $T_x = T_2 x^\psi$ with T_2 the temperature of the fire-ball at radius r_2 . In Fig. 3, we show the dependence of W on the ratio r_1/r_2 for the case $\Gamma \gg 1$ and $\psi = 2/3, 0.8$ and 1.0 . If the time-averaged spectrum is obtained for a time step Δ consecutively over the entire burst, then the radius of the fire-ball after $n\Delta$ duration can be expressed in terms of the initial radius of the burst (r_0) as

$$r_n = n\beta c\Delta\Gamma^2 + r_0$$

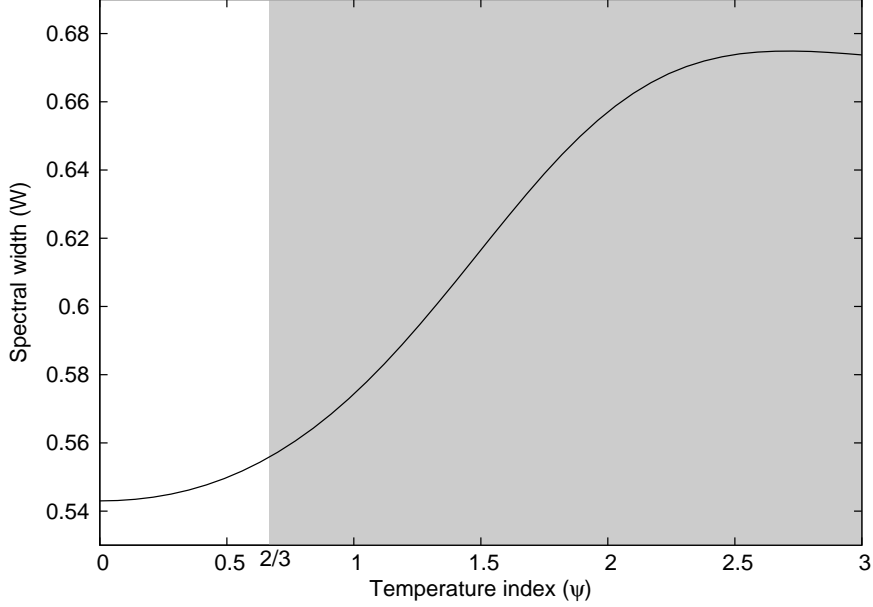


Figure 2: Variation of the instantaneous spectral width W with respect to ψ

The ratio of the radii falling on the beginning and the end of Δ will then be

$$\frac{r_n}{r_{n+1}} = 1 - \frac{1}{n + 1 + \xi} \quad (5)$$

where, $\xi = \frac{r_0}{\beta c \Delta \Gamma^2}$. Since the ratio of the radii continuously evolves during a burst, the width of the time-averaged spectrum will additionally depend on the initial burst radius r_0 and the time segment n , along with Γ and ψ . From equation (5), the minimum value of the ratio of radii attained will be 0.5 corresponding to $\xi = 0$ and $n = 1$, which approaches to 1 as n increases. Hence, W will eventually attain a constant value with negligible change soon after the explosion. The light curve of the burst can be obtained by integrating equation (4) over the frequency range of interest. The duration of the burst (τ_{90}) can then be obtained by clipping the light curve at 5% of the total flux in the beginning and the end of the burst.

3. Spectral width of Long Bursts

To study the maximum attainable width of long GRBs under the expanding fire-ball scenario, we obtain one second time-averaged light curve integrated over the energies 8 keV to 40 MeV, consistent with the observations (Axelsson & Borgonovo, 2015). In Fig. 4, we show the evolution

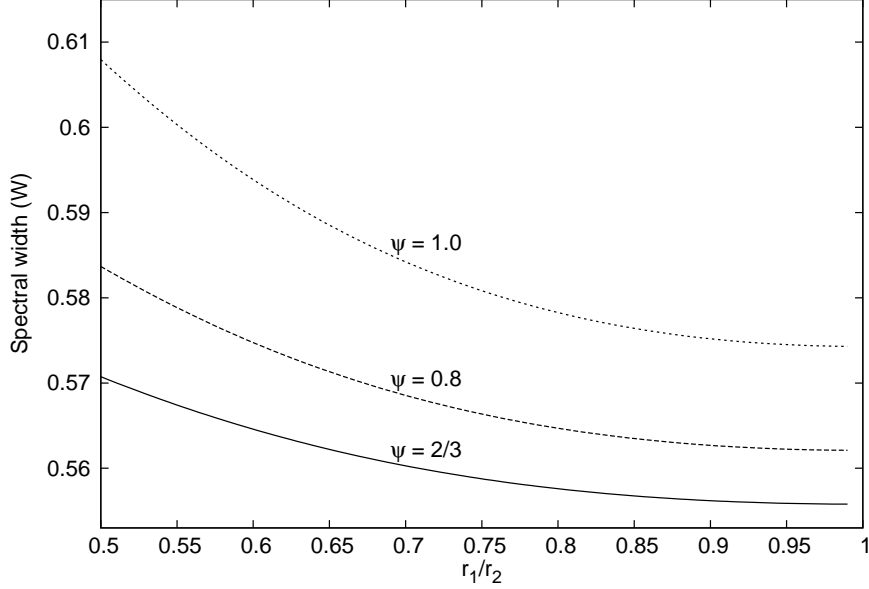


Figure 3: Variation of the time-averaged spectral width W with respect to the ratio of initial and final radius r_1/r_2 corresponding to the time segment, for $\psi = 2/3, 0.8$ and 1.0 .

of the normalized flux, time-averaged spectral width W and temperature corresponding to $\Gamma = 500$ and $T_0 = 10$ keV. The parameters ψ and ξ are chosen to be $(2/3, 1.5 \times 10^{-5})$, $(0.8, 1.85 \times 10^{-4})$ and $(1.0, 2.18 \times 10^{-3})$ such that $\tau_{90} \approx 30$ s, the typical duration of long GRBs. We find that the choice of ψ significantly varies the temporal profile, with the burst peaking earlier for smaller ψ values. For a given ψ , the burst peak time (t_{peak}) can be elongated by increasing ξ ; nevertheless, this will also increase the τ_{90} from the desired value.

The spectral width W can be as large as ~ 0.6 , during the initial phase of the burst; however, it rapidly decreases to a nearly constant value due to increase in ratio of radii $\frac{r_n}{r_{n+1}}$. Maintaining a constant τ_{90} , the width of the spectrum during the flux peak (W_p) increases with ψ and, in principle, can be adjusted to obtain the desired value ≈ 1.07 . For example, choosing $\xi = 0.31$, $\Gamma = 600$ and $\psi = 2.14$, we obtain $W_p \approx 1$ while $\tau_{90} \approx 30$ s; however, such choices will cause the burst to peak much earlier ($t_{peak} < 1$ s), inconsistent with the observations. Reduction of ψ to the adiabatic limiting value $2/3$ reduces W_p and this should be associated with a decrease in initial radius r_0 in addition, to maintain τ_{90} at the desired value.

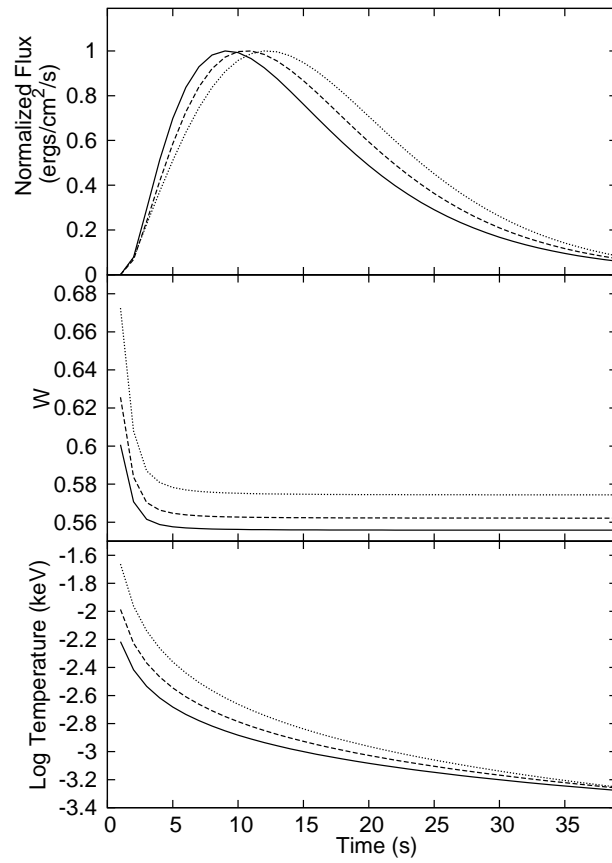


Figure 4: The evolution of the normalized flux (top), time-averaged spectral width W (middle) and temperature (bottom) corresponding to $\Gamma = 500$ and $T_0 = 10\text{keV}$ for $\psi = 2/3$ (bold), 0.8 (dashed) and 1.0 (dotted)

For a comparative study between the fire-ball parameters and the derived quantities of the burst, we study the variation of W_p and τ_{90} with respect to ψ and Γ . In Fig. 5a and 5b, we show the variation of W_p , τ_{90} and t_{peak} with ψ for $\Gamma = 200$ (solid), 500(dashed) and 800(dotted). The value of ξ is chosen to be 10^{-4} and T_0 is fixed at 10 keV. For a given Γ , W_p increases with ψ and sharply beyond $\psi \sim 0.8$. However, this is also associated with a significant decline in τ_{90} and t_{peak} (gray lines). In Fig. 5c and 5d, we again show the variation of W_p , τ_{90} and t_{peak} with respect to Γ for $\psi = 0.6$ (solid), 0.7 (dashed) and 0.8 (dotted). Here, larger Γ is associated with delayed t_{peak} and hence narrower W_p (see Fig. 4). Hence, requirement of a broader W_p demands a larger ψ and a smaller Γ which on the other hand shortens the burst duration as well as deviate largely from the adiabatic limit. This enforces a limit on maximum attainable width under the assumed fire-ball scenario and significantly hampers to achieve the width (1.07) demanded by the observations. Through the present study, we found that with an optimal choice of parameters and $\psi = 2/3$, maintaining τ_{90} and t_{peak} at a reasonable values corresponding to long GRBs, one can only attain $W_p \lesssim 0.557$ (e.g. $W_p \approx 0.557$ with $\tau_{90} \approx 20$ s and $t_{peak} \approx 5$ s for $\Gamma = 100$ and $\xi = 1.12 \times 10^{-4}$ and $\psi = 2/3$).

4. Summary & Discussion

The FWHM spectral width of the Band spectrum used to fit the time resolved spectrum of long GRBs is observed to be ≈ 1.07 . This is larger than the width of the simple blackbody spectrum defined by a Planck's function and smaller than the synchrotron spectrum from a Maxwellian/power-law distribution of electrons (Axelsson & Borgonovo, 2015). To understand the maximum attainable width under a simple fire-ball interpretation of GRB, we consider a scenario where the GRB emission to be a multi temperature blackbody distribution arising from a rapidly cooling and relativistically expanding fire-ball of hot thermal plasma. The dynamics of the fire-ball will cause the instantaneous spectrum to be broader than the simple blackbody spectrum with the emission from the higher latitudes hotter than the on-axis emission due to light travel time and relativistic effects. In addition, the time averaging of the emission will incorporate considerable evolution of the fire-ball and this will further broaden the emission. However, under this scenario, we are only able to obtain a maximum spectral width of ≈ 0.557 , while maintaining the burst duration to be

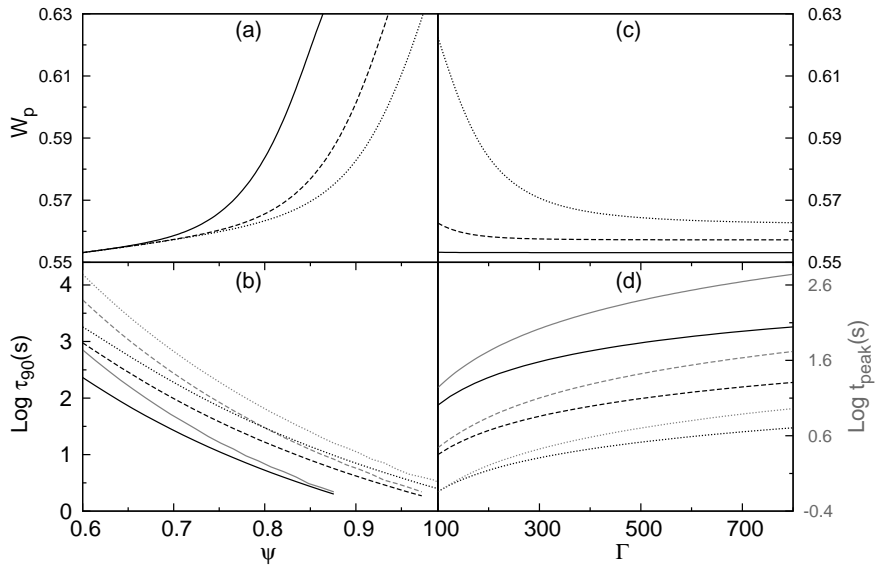


Figure 5: Left (a) and (b): Variation of the spectral width during the burst peak, W_p (a), and τ_{90} (b) with respect to ψ for $\Gamma = 200$ (solid), 500 (dashed) and 800 (dotted). Right (c) and (d): Variation of the spectral width during the burst peak, W_p (c), and τ_{90} (d) with respect to Γ for $\psi = 0.6$ (solid), 0.7 (dashed) and 0.8 (dotted). Gray lines in (b) and (d) indicate the burst peak time t_{peak} .

consistent with the long GRBs. This is marginally broader than the simple blackbody spectrum but significantly smaller than the observed values.

In this work, we highlight the inadequacy of a simple fire-ball model to explain the observed large spectral width of the GRB prompt emission. A plausible explanation for this may include the emission from the sub-photospheric region. The last scattering position of the trapped photons may not be necessarily associated with the photosphere, rather can emerge from regions beneath it (Beloborodov, 2010; Pe'er, 2008). Hence, the emission could be from an extended volume instead of a simple surface which can significantly broaden the observed spectrum. Alternatively, the expansion velocity of the fire-ball may not be isotropic, instead depend on the opening angle (Lundman, Pe'er, & Ryde, 2013). Such stratification of flow velocity can include emission from higher latitudes (i.e beyond the opening angle $1/\Gamma$ of a uniformly expanding fire-ball) which can further broaden the observed spectrum.

References

- Abramowicz M. A., Novikov I. D., Paczynski B., 1991, *ApJ*, 369, 175
Axelsson M., et al., 2012, *ApJ*, 757, L31
Axelsson M., Borgonovo L., 2015, *MNRAS*, 447, 3150
Band D., et al., 1993, *ApJ*, 413, 281
Basak R., Rao A. R., 2014, *MNRAS*, 442, 419
Bégué D., Vereshchagin G. V., 2014, *MNRAS*, 439, 924
Bhat P. N., et al., 2016, *ApJS*, 223, 28
Beloborodov A. M., 2010, *MNRAS*, 407, 1033
Blinnikov S. I., Kozyreva A. V., Panchenko I. E., 1999, *Astronomy Reports*, 43, 739
Burgess J. M., et al., 2014, *ApJ*, 784, L43
Burgess J. M., Ryde F., 2015, *MNRAS*, 447, 3087
Costa E., et al., 1997, *Nature*, 387, 783
Crider A., et al., 1997, *ApJ*, 479, L39
Daigne F., Mochkovitch R., 1998, *MNRAS*, 296, 275
Dezalay J. P., et al., 1996, *ApJ*, 471, L27
Eichler D., Livio M., Piran T., Schramm D. N., 1989, *Nature*, 340, 126
Ghirlanda G., Celotti A., Ghisellini G., 2003, *A&A*, 406, 879
Goodman J., 1986, *ApJ*, 308, L47

- Guiriec S., Fermi/GBM Collaboration, 2010, Bulletin of the American Astronomical Society, 42, 654
- Guiriec S., et al., 2013, ApJ, 770, 32
- Kobayashi S., Piran T., Sari R., 1997, ApJ, 490, 92
- Kouveliotou C., et al., 1993, ApJ, 413, L101
- Kouveliotou C., et al., 1996, AIPC, 384, 42
- Lundman C., Pe'er A., Ryde F., 2013, MNRAS, 428, 2430
- MacFadyen A. I., Woosley S. E., 1999, ApJ, 524, 262
- Paczynski B., 1986, ApJ, 308, L43
- Paczynski B., 1991, A&A, 41, 257
- Panaitescu A., Meszaros P., 1998, ApJ, 526, 707
- Pe'er A., 2008, ApJ, 682, 463
- Pe'er A., 2015, AdAst, 2015, 907321
- Pe'er A., Ryde, F., 2016, arXiv:1603.05058
- Piran T., Shemi A., Narayan R., 1993, MNRAS, 263, 861
- Piran T., 2004, RvMP, 76, 1143
- Preece R. D., et al., 1998, ApJ, 506, L23
- Rao A. R., et al., 2014, RAA, 14, 35-46
- Rosswog S., Piran T., Nakar E., 2013, MNRAS, 430, 2585
- Ryde F., 2004, ApJ, 614, 827
- van Paradijs J., et al., 1997, Nature, 386, 686
- Vedrenne G., Atteia J.-L., 2009, Gamma-Ray Bursts: The Brightest Explosions in the Universe, Springer Praxis Books. Springer, Berlin, Heidelberg
- Woosley S. E., 1993, ApJ, 405, 273
- Yu H.-F., et al., 2015, A&A, 583, A129
- Zhang B., Yan H., 2011, ApJ, 726, 90

Appendix A. Instantaneous thermal spectrum from the expanding fire-ball

Let r_0 be the instantaneous radius of the fire-ball. For an observer located at a distance D , the emission from r_0 will coincide the emission from higher latitude (θ) at an earlier radius $r_{0\theta}$ due to light travel time effects (Fig. A.6). If the expansion velocity is βc (c being the speed of light), then

$$r_{0\theta} = r_0 \left[\frac{(1 - \beta)}{(1 - \beta \cos \theta)} \right] \quad (\text{A.1})$$

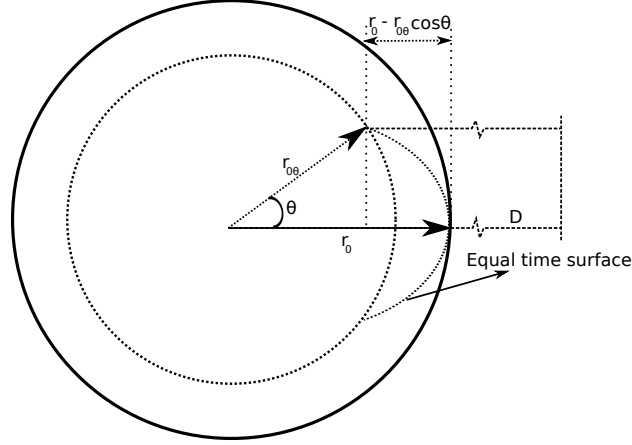


Figure A.6: Schematic representation indicating the light travel time effects on the instantaneous spectrum seen by a distant observer.

The net flux at frequency ν emitted from the surface of the fire-ball will then be

$$F_\nu = \frac{2\pi r_0^2 \Gamma^3}{D^2} (1 - \beta)^2 \int_\beta^1 I_{\nu'} \left(\frac{1 + \beta\mu}{1 - \beta\mu} \right)^3 (\mu - \beta) \mu d\mu \quad (\text{A.2})$$

Here, $\mu = \cos\theta$, $I_{\nu'}$ is the specific intensity measured in the rest frame of the ejecta and $\nu' = \nu[\Gamma(1 + \beta\mu)]^{-1}$. For thermal emission, $I_{\nu'}$ can be replaced by the Planck function and we get

$$F_\nu = \frac{4\pi h}{c^2} \frac{r_0^2}{D^2} (1 - \beta)^2 \nu^3 \int_\beta^1 \frac{\mu d\mu}{\left\{ \exp \left[\frac{h\nu}{\Gamma k T_{0\theta} (1 + \beta\mu)} \right] - 1 \right\}} \frac{(\mu - \beta)}{(1 - \beta\mu)^3} \quad (\text{A.3})$$

where, $T_{0\theta}$ is the temperature corresponding to radius $r_{0\theta}$, h is the Planck constant and k is the Boltzmann constant. Using equation (1) and (A.1), $T_{0\theta}$ can be expressed as

$$T_{0\theta} = T_0 \left(\frac{1 - \beta\mu}{1 - \beta} \right)^\psi \quad (\text{A.4})$$

and equation (A.3) can be written as

$$f_\nu(r_0) = \frac{4\pi h}{c^2} \frac{r_0^2}{D^2} (1 - \beta)^2 \nu^3 \int_\beta^1 \frac{\mu d\mu}{\left\{ \exp \left[\frac{h\nu}{\Gamma k T_0 (1 + \beta\mu)} \left(\frac{1 - \beta}{1 - \beta\mu} \right)^\psi \right] - 1 \right\}} \frac{(\mu - \beta)}{(1 - \beta\mu)^3} \quad (\text{A.5})$$